Synthesis and Photovoltaic Properties of Low-Bandgap 4,7-Dithien-2-yl-2,1,3-Benzothiadiazole-Based Poly(heteroarylenevinylene)s

SHANPENG WEN, JIANING PEI, PENGFEI LI, YINHUA ZHOU, WEIDONG CHENG, QINGFENG DONG, ZAIFANG LI, WENJING TIAN

State Key Laboratory of Supramolecular Structure and Materials, Jilin University, Changchun 130012, People's Republic of China

Received 16 February 2011; accepted 1 April 2011
DOI: 10.1002/pola.24704
Published online 27 April 2011 in Wiley Online Library (wileyonlinelibrary.com).

ABSTRACT: Three novel low-bandgap copolymers containing alkylated 4,7-dithien-2-yl-2,1,3-benzothiadiazole (HBT) and different electron-rich functional groups (dialkylfluorene (PFV-HBT), dialkyloxyphenylene (PPV-HBT) and dialkylthiophene (PTV-HBT)) were prepared by Horner polycondensation reactions and characterized by ^{1}H NMR, gel permeation chromatography, and elemental analysis. The alkyl side chain brings these polymeric materials good solubility in common organic solvents, which is critical for the manufacture of solar cells in a cost-effective manner. The copolymers exhibit low optical bandgap from 1.48 to 1.83 eV. The highest occupied molecular orbital (HOMO) and lowest unoccupied molecular orbital (LUMO) energy levels of the copolymers were measured by cyclic voltammetry. Theoretical calculations revealed that the variation laws of HOMO and the LUMO energy levels are well consistent with cyclic voltammetry measurement. The bulk heterojunction photovoltaic devices with the structure of ITO/PEDOT-PSS/polymer:PCBM/LiF/Al were fabricated by using the three copolymers as the donor and (6,6)-phenyl-C_{61}-butyric acid methyl ester (PCBM) as the acceptor in the active layer. The device based on PTV-HBT:PCBM (1:4 w/w) achieved a power conversion efficiency of 1.05% under the illumination of AM 1.5, 100 mW/cm^2. © 2011 Wiley Periodicals, Inc. J Polym Sci Part A: Polym Chem 49: 2715–2724, 2011

KEYWORDS: bulk heterojunction; conducting polymers; copolymerization; electrochemistry; polymer solar cells

INTRODUCTION Polymer solar cells (PSCs) have great potential as the future energy source due to the advantages of low cost, easy processing, light weight, being mechanically flexible, and suitable for large-area fabrication.[1–6] The most widely used configuration of PSCs is the bulk heterojunction (BHJ) solar cells in which the active layer consists of a blend of an electron donating conjugated polymer and an electron acceptor such as (6,6)-phenyl C_{61}-butyric acid methyl ester (PCBM).[7–10] Recently, such polymer photovoltaic cells with power conversion efficiency (PCE) as high as 5% have been realized by using a blend of regioregular poly(3-hexylthiophene) (P3HT) and PCBM as the active layer.[11,12] However, further improvement of P3HT-based PVC devices is difficult due to P3HT's intrinsic absorption limit. A good overlap of the absorption of the active layer with the solar spectrum [visible and near-infrared (IR)] is required to improve the overall solar cell energy conversion efficiency.[13] Low band gap materials that absorb visible to IR light are favorable in the selection of the active layer materials. In the past few years, chemists have synthesized various low-bandgap polymers consisting of alternating electron donating (D) and electron accepting (A) units being able to harvest more photons at long wavelengths.[14]

Intramolecular charge transfer (ICT) interaction between the donor and acceptor units within D-A copolymers facilitates the manipulation of the optical properties and electronic structures (the highest occupied molecular orbital (HOMO) and lowest unoccupied molecular orbital (LUMO) energy levels, and bandgaps). Thus, through the design and selection of D and A building blocks, the strength of ICT can be tuned, allowing D-A copolymers to exhibit low band gap and broad absorption band that extends to the red and even IR region. By using this strategy, many novel low band gap polymers have been synthesized and used in PSCs with PCEs over 7% combined with intensive device engineering efforts.[15]

Among the large variety of acceptor segments, 4,7-dithien-2-yl-2,1,3-benzothiadiazole (DTBT), linking two thienyl units in the 4,7-position of 2,1,3-benzothiadiazole, has been developed and copolymerized with many types of donor segments, such as fluorene,[16] silafluorene,[17] dialkoxyphenylene,[18] carbezole,[19] dithienosilole,[20] cyclopenta[2,1-b:3,4-b]dithiophene,[21] and benzo[1,2-*b*:4,5-*b*′]dithiophene.[22] The two thiophene units were added on both ends of the 2,1,3-benzothiadiazole to obtain relatively planar copolymers with good charge transport properties.[23] Interestingly, this type of polymers has recently reached a PCE of 6.1% in BHJ photovoltaic devices.[24]

Link pattern (e.g., carbon-carbon single, double, or triple bond) has a significant influence on the chemical and physical properties of polymers.[25,26] Generally, low-bandgap

Correspondence to: W. Tian (E-mail: wjtian@jlu.edu.cn)

DTBT-based copolymers have been synthesized using the linkage of single bonds via Suzuki or Stille cross-coupling reaction, while the alternative copolymer linked by double bonds via Horner reaction that bear DTBT units is still unexplored. The advantage of incorporating double bond, vinylene, linkages between the donor and acceptor groups inside the conjugated copolymers is that the vinylene linkage can increase the planarity of the copolymer backbone by eliminating torsional interactions between donor and acceptor rings, thus extend the conjugation length and decrease the bandgap of the copolymers.[27]

Herein, we synthesized three new π-conjugated copolymers consisting of alkylated 4,7-dithien-2-yl-2,1,3-benzothiadiazole (HBT) acceptor unit coupled to different electron-donating moieties: poly(fluorenevinylene-alt-4,7-dithien-2-yl-2,1,3-Benzothiadiazole) (PFV-HBT), poly(phenylenevinylene-alt-4,7-dithien-2-yl-2,1,3-benzothiadiazole) (PPV-HBT), and poly(-thiophenevinylene-alt-4,7-dithien-2-yl-2,1,3-benzothiadiazole) (PTV-HBT). We reasoned that the incorporation of functional electron-donating moieties into the HBT-based copolymers with different electron-donating ability will bring various degrees of ICT to the conjugated system to provide a means of tuning the HOMO/LUMO energy levels and the bandgaps. Indeed, we found that the energy level and absorption spectra of the copolymers can be fine-tuned by changing the moieties with different electron-donating ability. The photovoltaic cells based on these three copolymers, PFV-HBT, PPV-HBT, and PTV-HBT with a cell structure of ITO/PEDOT/copolymer:PCBM/LiF/Al exhibit PCE of 0.33, 0.47, and 1.05% respectively under one sun of AM 1.5 solar simulator illumination (100 mW/cm^2).

EXPERIMENTAL

Materials

All starting materials were purchased from either Acros or Aldrich Chemical Co. and used without further purification, unless otherwise noted. In synthetic preparations, diethyl ether and THF were dried by distillation from sodium/benzophenone under nitrogen. Similarly, DMF and dichloromethane were distilled from CaH_2 under nitrogen. 4,7-dibromo-2,1,3-benzothiadiazole,[28] 2,7-Bis(methylenediethyl phosphate)-9,9-di-*n*-octylfluoene (M-2), 2-Methoxy-5-(2-ethylhexyloxy)-1,4-xylylenebis(diethylphosphonate) (M-3) and 3,4-Dihexyl-2,5-bis(methylenediethyl phosphate)thiophene (M-4)[29] were prepared according to known literature procedures.

Measurements and Characterization

^{1}H NMR spectra were recorded on Bruker AVANCE 500-MHz spectrometer with chloroform-d as solvent and tetramethylsilane (TMS) as internal standard. The elemental analysis was carried out with a Thermoquest CHNS-Ovelemental analyzer. The gel permeation chromatographic (GPC) analysis was carried out with a Waters 410 instrument with tetrahydrofuran as the eluent (flowrate: 1 mL/min, at 35 °C) and polystyrene as the standard. The thermogravimetric analysis (TGA) was performed on a Perkine Elmer Pyris 1 analyzer under nitrogen atmosphere (100 mL/min) at a heating rate of 10 °C/min. UV-visible absorption spectra were measured using a Shimadzu UV-3600 spectrophotometer. Electrochemical measurements of these derivatives were performed with a Bioanalytical Systems BAS 10 B/W electrochemical workstation.

Photovoltaic Device Fabrication and Characterization

The solar cells were fabricated with a device structure ITO/PEDOT:PSS/Polymer:PCBM Blend/LiF/Al. The ITO glass substrates were precleaned by detergent, acetone, and boiling in H_2O_2. Highly conducting poly(3,4-ethylenedioxythiophene):-poly(sty-enesulfonate) (PEDOT:PSS, Baytron P, Al4083) was spin-casted (3000 rpm) at a thickness of $\sim$ 40 nm from aqueous solution (after passing through a 0.45 μm filter). The substrate was annealed at 120 °C for 15 min on hot plate. The active layer contained a blend of copolymers as electron donor and PCBM as electron acceptor, which was prepared by weight ratio (1:1, 1:2, 1:3, and 1:4 w/w) in chlorobenzene (5 mg/mL) for copolymers. The active layers were obtained by spin coating the blend solutions at 1000 rpm for 50 s and the thickness of films was $\sim$ 90 nm, as measured with the Ambios Technology XP-2. Subsequently, LiF (0.6 nm) and Al (100 nm) electrodes were deposited via thermal evaporation in vacuum (5×10^{-4} Pa). The active area was about 5 mm^2. Current-voltage (*J-V*) characteristics were recorded using Keithley 2400 Source Meter in the dark and under 100 mW/cm^2 simulated AM 1.5 G irradiation (Sciencetech SS-0.5K Solar Simulator). All the measurements were performed under ambient atmosphere at room temperature.

Synthesis of the Monomer

3-Hexylthiophene (1)

Mg (1.20 g, 50 mmol) was placed in 10 mL of dry ether then cooled to 0 °C. Hexylbromide (9.2 mL, 65 mmol) was added dropwise over 2 h, and the reaction mixture was stirred for another hour. This solution was then transferred slowly via a cannula to a mixture of 3-bromothiophene (2.36 mL, 21 mmol) and 50 mg of Ni(dppp)Cl_2 in 50 mL of dry ether while cooling on ice. The reaction mixture was stirred for 16 h at room temperature and subsequently poured out in 500 mL of ice/water containing 10 mL of concentrated HCl. The product was extracted with ether and the combined organic layers were washed with plenty of water and brine, successively. The organic extracts were dried over anhydrous $MgSO_4$, evaporated, and purified with column chromatography on silica gel with petroleum ether as the eluant to give **1** colorless oil 2.18 g (yeild 72%).

^{1}H NMR (500 MHz, $CDCl_3$, TMS): δ (ppm) 7.23 (dd, 1H), 6.95–6.90 (m, 2H), 2.62 (t, J = 7.5 Hz, 2H), 1.65–1.58 (m, 2H), 1.35–1.24 (m, 6H), 0.88 (t, J = 7.0 Hz, 3H). Anal. Calcd for $C_{10}H_{16}S$: C, 71.37; H, 9.58. Found: C, 71.21; H, 9.73.

4-(Hexyl-2-thienyl)stannane (2)

To a solution of 3-hexylthiophene (1.8 g, 12.50 mmol) in anhydrous THF (40 mL) at −78 °C, n-BuLi (5.5 mL, 13.75 mmol) was added dropwise, and the mixture was stirred at this temperature under a nitrogen atmosphere for 2 h. Then tributylchlorostannane (4.0 mL, 15.00 mmol) was added, and the mixture was stirred at −30 °C for 12 h. The mixture was

poured into saturated aqueous $NaHCO_3$, and the organic phase was separated and washed with saturated aqueous brine and then dried over an anhydrous sodium sulfate. The solvent was removed at a reduced pressure, and the residue was purified with column chromatography on neutral alumina with petroleum ether as the eluant to give **2** colorless oil 4.3 g (yeild 76%).

^{1}H NMR (500 MHz, $CDCl_3$, TMS): δ (ppm) 7.11 (s, 1H), 6.89 (s, 1H), 2.57 (t, J = 8.0, 2H), 1.58–1.43 (m, 8H), 1.30–1.15 (m, 12H), 1.10–0.92 (m, 6H), 0.81 (t, J = 7.0 Hz, 12H). Anal. Calcd for $C_{22}H_{42}SSn$: C, 57.78; H, 9.26. Found: C, 57.56; H, 9.42.

4,7-Di(4-hexyl-2-thienyl)-2,1,3-benzothiadiazole (4)

To a solution of 4,7-dibromo-2,1,3-benzothiadiazole (**3**) (1.91 g, 6.50 mmol) and compound **2** (6.84 g, 14.95 mmol) in THF (60 ml), $PdCl_2(PPh_3)_2$ (137 mg, 3 mol %) was added. The mixture was refluxed under a nitrogen atmosphere for 12 h. After removal of the solvent under reduced pressure, the residue was purified by column chromatography on silica gel (petroleum ether/CH_2Cl_2, 15:1). Recrystallization from ethanol gave the title compound **4** (2.68 g, 82.5%) as red solid.

^{1}H NMR (500 MHz, $CDCl_3$, TMS): δ (ppm) 7.98 (s, 2H), 7.83 (s, 2H), 7.04 (s, 2H), 2.69 (t, J = 7.5 Hz, 4H), 1.74–1.67 (m, 4H), 1.42–1.25 (m, 12H), 0.89 (t, J = 6.5 Hz, 6H). Anal. Calcd for $C_{26}H_{32}N_2S_3$: C, 66.62; H, 6.88. Found: C, 66.73; H, 6.74.

5,5′-(2,1,3-benzothiadiazole-4,7-diyl-)bis (3-hexylthiophene-2-carbaldehyde) Monomer (M-1)

DMF (45 mL, excess) and phosphorous oxychloride ($POCl_3$) (10 mL, excess) were mixed together and stirred for 30 min at 0 °C. To the yellow DMF–$POCl_3$ complex, a solution of 4 (2.00 g, 4.00 mmol) in DMF (10 mL) was added dropwise at 0 °C. The reaction mixture was heated at 95 °C for 24 h under nitrogen. Then, the reaction mixture was poured into dilute HCl solution (150 mL), and the organic layers were extracted with chloroform. The organic layer was washed with an aqueous solution of $NaHCO_3$ and subsequently with distilled water. After drying over $MgSO_4$ and removal of organic solvent under reduced pressure, the crude product was purified by column chromatography (petroleum ether/ethyl acetate, 10:1) to provide 1.74 g (78%) of the title product as a red solid.

^{1}H NMR (500 MHz, $CDCl_3$, TMS): δ (ppm) 10.12 (s, 2H), 8.10 (s, 2H), 8.01 (s, 2H), 3.05 (t, J = 8.0, 4H), 1.81–1.74 (m, 4H), 1.47–1.21 (m, 12H), 0.89 (t, J =6.5 Hz, 6H). Anal. Calcd for $C_{28}H_{32}N_2O_2S_3$: C, 64.09; H, 6.15. Found: C, 63.92; H, 6.21.

SYNTHESIS OF THE POLYMERS

General Procedure for Horner-Wadsworth-Emmons Polycondensation

Poly(fluorenevinylene-alt-4,7-dithien-2-yl-2,1,3-benzothiadiazole) (PFV-HBT)

The dicarboxyaldehyde (M-1) (0.223 g, 0.40 mmol) and monomer (M-2) (0.28 g, 0.40 mmol) were dissolved in 20 mL anhydrous THF under nitrogen. To this solution, potassium tertbutoxide (2 mL of a 1 M solution in THF) was added. The reaction was stirred for 48 h at room temperature under nitrogen. The polymer was precipitated into 300 mL of methanol and filtered through a Soxhlet thimble, which was then subjected to Soxhlet extraction with methanol, hexane, acetone, and chloroform. The fraction from chloroform was concentrated under reduced pressure and precipitated into methanol (200 mL), collected by filtration. The final product was dried under vacuum overnight to afford PFV-HBT as a black solid (0.27 g, 75%).

TABLE 1 Polymerization Results and Thermal Properties of Copolymers

Polymer	Yield (%)	M_n (10^3)	M_w (10^3)	PDI	TGA (T_d)
PFV-HBT	75	3.32	4.29	1.29	279
PPV-HBT	72	4.10	6.37	1.64	283
PTV-HBT	81	7.09	9.98	1.41	298

^{1}H NMR (500 MHz, $CDCl_3$, TMS): δ (ppm) 7.92 (br, 2H, -benzothiadiazole), 7.80 (br, 2H, -Th), 7.64–7.28 (m, 6H,), 7.09–6.94 (m, 4H, -vinylic), 2.78–2.65 (m, 4H, -CH_2-), 2.00–1.87 (m, 4H), 1.42–0.80 (m, 42H), 0.76–0.72 (m, 6H), 0.57 (br, 4H). Anal. Calcd for $(C_{59}H_{74}N_2S_3)$n: C, 78.09; H, 8.22. Found: C, 77.76; H, 8.38.

Similarly, the monomer M-3, M-4, and dicarboxyaldehyde (M-1) were polymerized using potassium tert-butoxide to obtain the polymers poly(phenylenevinylene-alt-4,7-dithien-2-yl-2,1,3-benzothiadiazole) (PPV-HBT), poly(thiophenevinylene-alt-4,7-dithien-2-yl-2,1,3-benzothiadiazole) (PTV-HBT). The yield and molecular weights of the polymers are summarized in Table 1.

PPV-HBT, 72%, ^{1}H NMR (500 MHz, $CDCl_3$, TMS): δ (ppm) 8.03–7.95 (m, 2H, benzothiadiazole), 7.83 (br, 2H, -Th), 7.52–7.28 (m, 2H, -Ph), 7.11–6.95 (m, 4H, -vinylic), 4.06–3.86 (m, 5H, -OCH_2- and -OCH_3), 2.77 (br, 4H, -CH_2-), 1.88–0.81 (m, 37H). Anal. Calcd for $(C_{46}H_{56}N_2O_2S_3)$n: C,71.76; H, 7.49. Found: C, 70.95; H, 7.89.

PTV-HBT, 81%, ^{1}H NMR (500 MHz, $CDCl_3$, TMS): δ (ppm) 7.99 (br, 2H, -benzothiadiazole), 7.81 (br, 2H, -Th), 7.15–6.80 (m, 4H, -vinylic), 2.82–2.45 (m, 8H, -CH2-), 1.74–1.28 (m, 32H, -CH_2-), 0.91 (br, 12H, -CH_3). Anal. Calcd for $(C_{46}H_{60}N_2S_4)$n: C, 71.82; H, 7.86. Found: C, 71.34; H, 8.23.

RESULTS AND DISCUSSION

Synthesis and Characterization

Synthetic routes of the monomers and copolymers are shown in Schemes 1 and 2. Monomer (M-1) was synthesized in a multistep synthesis. Starting from commercially available 3-bromothiophene, in two steps, 2-tributyltin-4-hexylthiophene (compound **2**) was synthesized from the reaction of the lithium salt of the 3-hexylthiophene with tributyltin chloride. This compound was used as starting material for the Stille cross-coupling reaction with 4,7-dibromo-2,1,3-benzothiadiazole (**3**) to provide compound **4**. Monomer (M-1) was obtained in good yield by using an excess of two equivalents

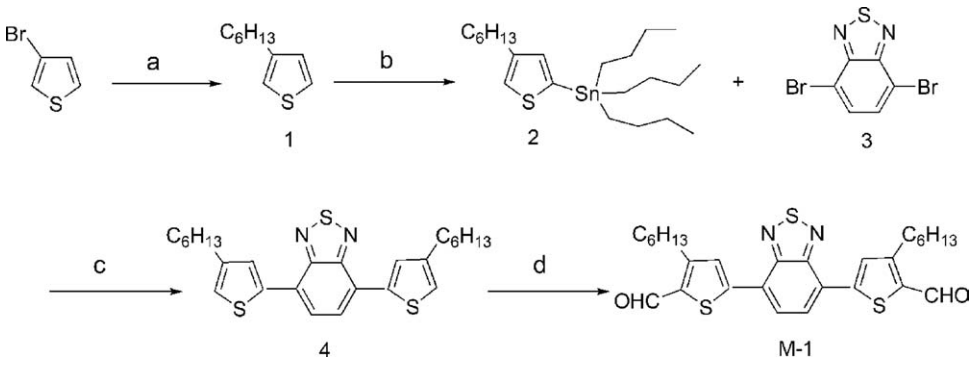

SCHEME 1 Syntheses of monomer M-1. Reagents and conditions: (a) (i) hexylbromide, diethyl ether, Mg; (ii) THF, $Ni(dppp)Cl_2$; (b) n-Buli, THF, tributylchlorostannane, −78 °C to −30 °C; (c) THF, $PdCl_2(PPh_3)_2$; (d) DMF, $POCl_3$, heated at 95 °C for 24 h.

of DMF/phosphoryl chloride reagent in the Vilsmeier reaction. In ^{1}H NMR spectra of M-1, as shown in Figure 1, thiophene proton peaked at about 7.04 ppm, disappeared after the Vilsmeier reaction, and a new peak appeared at about 10.12 ppm, which confirmed the success of the Vilsmeier reaction. The purity of the monomer (M-1) and the intermediate compounds were confirmed by ^{1}H NMR spectroscopy and elemental analysis. The phosphonate esters (M-2–M-4) were synthesized by Michaelis-Arbuzov reaction.[30] Monomers (M-2–M-4) were copolymerized with Monomer (M-1) by using the t-BuOK Horner coupling method. The yields of the resulting copolymers were over 70%. All the copolymers exhibited good solubility in common organic solvents such as chloroform, tetrahydrofuran, and chlorobenzene. In the ^{1}H NMR spectrum of PTV-HBT (Figure 1), the characteristic peaks at 8.02–7.88 ppm, 7.85–7.55 ppm, and 7.15–6.80 ppm can be assigned to the resonance of protons on the benzothiadiazole ring, the thiophene ring, and the vinylene group, respectively. The peaks due to protons in -CH_2- linked to the thiophene ring are at 2.82–2.45 ppm; the peaks at 1.74–0.91 ppm correspond to the protons of the long alkyl chain.

The molecular weights and polydispersities of the resulting copolymers were determined by GPC analysis with a polystyrene standard calibration. The weight-average molecular weights (Mw) of PFV-HBT, PPV-HBT, and PTV-HBT were 4.3 × 10^3, 6.4 × 10^3, and 10 × 10^3 with PDIs (polydispersity index, M_w/M_n) of 1.29, 1.64, and 1.41, respectively. Table 1 summarizes the polymerization results including molecular weights, PDI, and thermal stability of the copolymers.

Thermal Properties

Figure 2 shows the TGA curves of the synthesized copolymers at the heating rate of 10 °C/min under a nitrogen atmosphere. As shown in Figure 2, the decomposition temperatures (T_d) of the copolymers are in the range of 279–298 °C, which suggests relatively good thermal stability. Obviously, the thermal stability of the copolymers is adequate for the fabrication processes of PSCs and other optoelectronic devices. The T_d of the copolymers is summarized in Table 1.

Optical Properties

The optical absorption spectra of PFV-HBT, PPV-HBT, and PTV-HBT in dilute (10^{-5} M) chloroform solution, and thin films are shown in Figure 3, and the main optical properties of the copolymers are listed in Table 2. PFV-HBT with the weak electron-donating dialkyfluorene moiety showed two absorption bands at 424 nm and 553 nm in dilute solution [Fig. 3(a)], which can be assigned to π-π^* transition of the

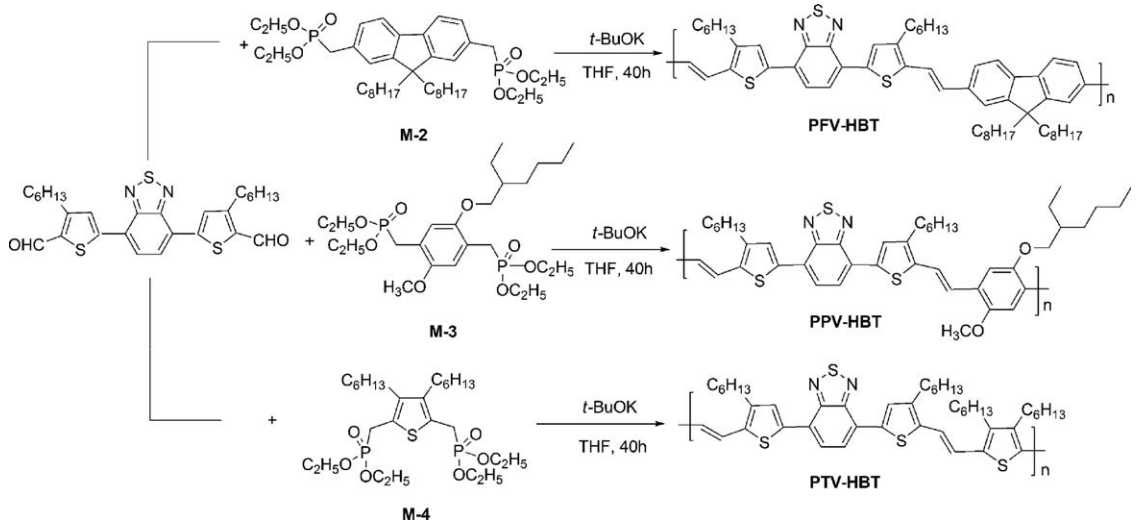

SCHEME 2 Syntheses of copolymers.

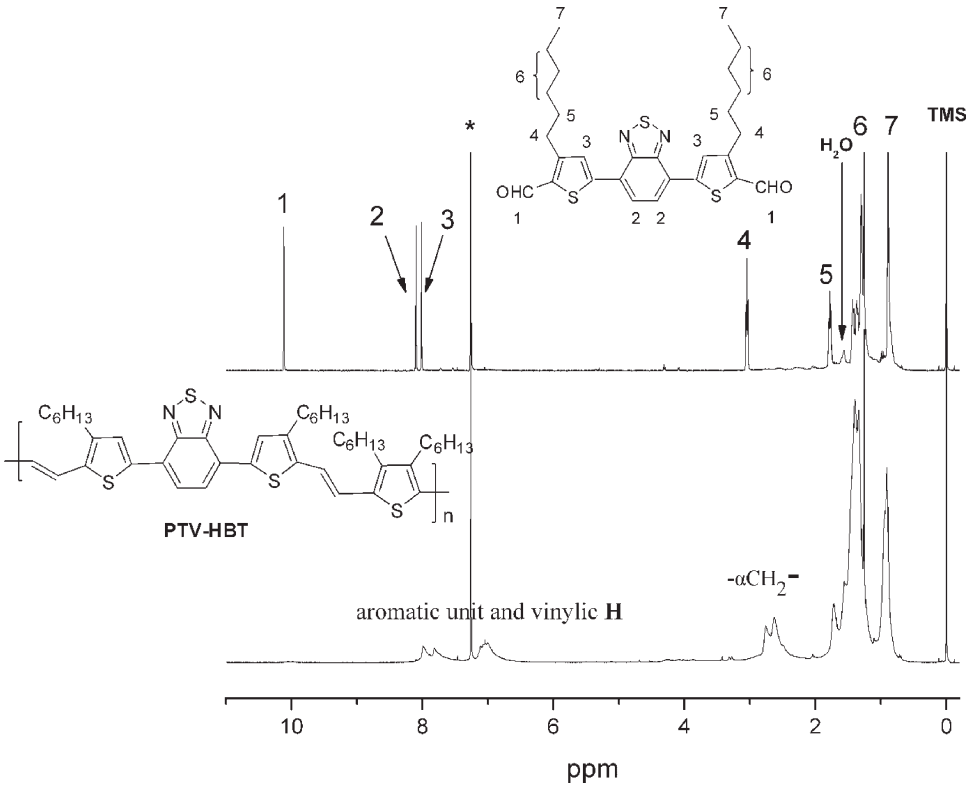

FIGURE 1 500 MHz-^{1}H NMR spectra of monomer M-1 and co-polymer PTV-HBT.

conjugated polymer backbone and ICT interaction between the fluorene donor and HBT-based acceptor.[31] Similarly, the absorption spectra of other copolymers (PPV-HBT and PTV-HBT) in dilute solutions also showed two bands near 451, 463 nm and 563, 653 nm due to the π-π* transition and the ICT interaction, respectively. The solution absorption spectrum of PTV-HBT, with an absorption maximum (λ_{max}^{abs}) at 653 nm, is red-shifted compared with those of PFV-HBT (λ_{max}^{abs} = 553 nm), and PPV-HBT (λ_{max}^{abs} = 563 nm), which can be explained by much stronger ICT effect in PTV-HBT than that in PFV-HBT and PTV-HBT. Among the three copolymers, there is an alternative "D*-(D-A-D)" structure, where D* is the donor with varied electron-donating ability and D-A-D is the HBT-based acceptor unit. The stronger electron-donating ability D* possesses, the higher electronic delocalization degree and the stronger ICT the copolymer has. Since the order of the electron-donating abilities of the three D* is dialkylthiophene > dialkyloxyphenylene > dialkylfluorene, the strongest electron-donating ability of thiophene compared with dialkylfluorene and dialkyloxyphenylene improves the effective conjugation length along polymer backbone, resulting in an increase in the ICT strength and thus electronic delocalization.

Figure 3(b) shows the optical absorption spectra of thin films of the copolymers. The thin film absorption spectra are generally similar in shape to those in dilute solution. The maximum absorption peak of PFV-HBT at visible region shows a 16 nm red shift between in solutions and thin films. In the case of PPV-HBT and PTV-HBT, the absorption spectra in thin films also exhibit 12 nm and 13 nm red shift, respectively, presumably indicating the formation of a π-stacked structure in the solid state.[32,33] From the low energetic edge of the absorption spectrum of the individual copolymer, the band gap of PFV-HBT was estimated to be 1.83 eV (λ_{max}^{abs} = 676 nm), while smaller band gaps of 1.64 eV and 1.48 eV were calculated for PPV-HBT and PTV-HBT (λ_{max}^{abs} = 757 nm and λ_{max}^{abs} = 835 nm), respectively. In comparison with similar copolymer PT3BT (without double bonds in the main chain, E_g^{opt} =1.59 eV), the absorption spectra of PTV-HBT was red-shifted (42 nm in thin film, E_g^{opt} =1.48 eV) due to higher planarity along the polymer backbone.[32(b)]

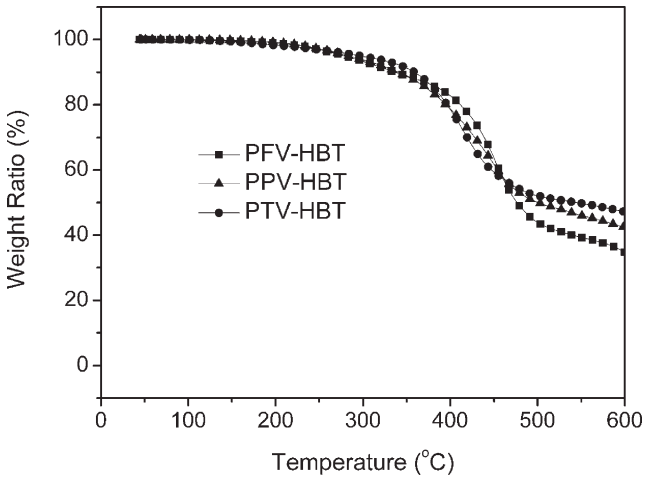

FIGURE 2 TGA curves of copolymers at the heating rate of 10 °C/min under nitrogen atmosphere.

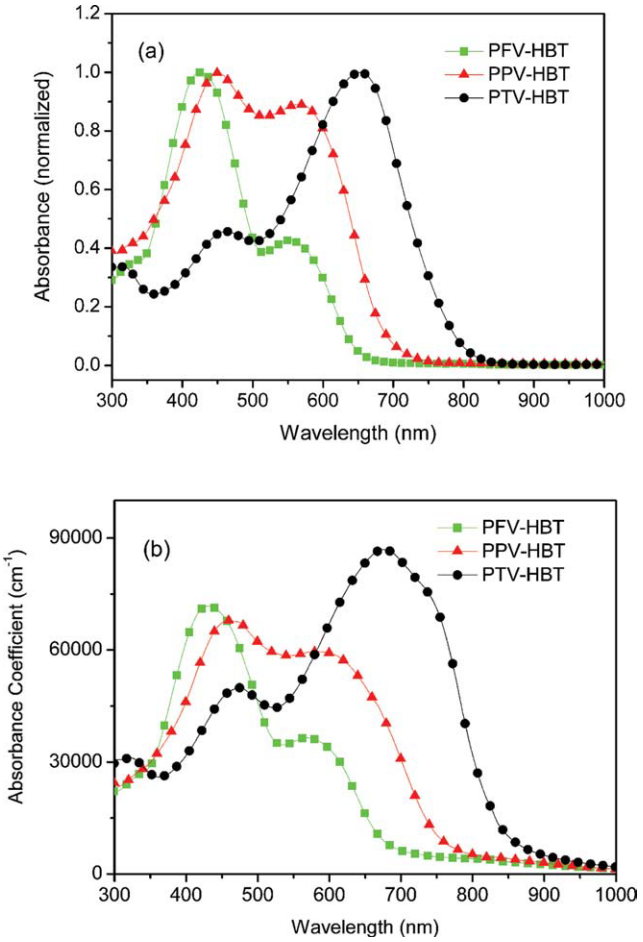

FIGURE 3 UV-vis absorption spectra of PFV-HBT, PPV-HBT, and PTV-HBT in chloroform solution and (b) in thin films. [Color figure can be viewed in the online issue, which is available at wileyonlinelibrary.com.]

Electrochemical Properties

Cyclic voltammetry of the copolymers in films was performed in acetonitrile with 0.1 M tetrabutylammonium hexafluorophosphate ($TBAPF_6$) as supporting electrolyte at scan rates of 50 mV/s. Platinum wire electrodes were used as both counter and working electrodes, and silver/silver ion (Ag in 0.1 M $AgNO_3$ solution, from Bioanalytical Systems) was used as a reference electrode. Ferrocene/ferrocenium (Fc/Fc^+) was used as the internal standard.

The cyclic voltammagram of the copolymers are shown in Figure 4. On the anodic sweep, all copolymers showed an oxidation with onset potentials of 0.54 V (versus Ag/Ag^+) for PFV-HBT, 0.34 V for PPV-HBT and 0.23 V for PTV-HBT, respectively. In contrast, the cathodic sweep showed onset reduction potentials of −1.42 V (versus Ag/Ag^+) for PFV-HBT, −1.42 V for PPV-HBT, and −1.41 V for PTV-HBT.

From the onset oxidation potentials (E_{ox}^{onset}) and the onset reduction potentials (E_{red}^{onset}) of the copolymers, HOMO and LUMO energy levels as well as the energy gaps were calculated according to the following equations,[29,34]

$$\mathrm{HOMO(eV)} = -\mathrm{e}(E_{ox}^{onset} + 4.73)$$

$$\mathrm{LUMO(eV)} = -\mathrm{e}(E_{red}^{onset} + 4.73)$$

$$E_g^{ec}\,\mathrm{(eV)} = \mathrm{e}(E_{ox}^{onset} - E_{red}^{onset})$$

where E_{ox}^{onset} and E_{red}^{onset} are the measured onset potentials relative to Ag/Ag^+.

The results of the electrochemical measurements and calculated energy levels of the copolymers are listed in Table 2. The estimated HOMO and LUMO energy levels of PFV-HBT are −5.27 and −3.31 eV, respectively. The LUMO energy levels of PPV-HBT and PTV-HBT are at −3.31 eV and −3.32 eV, respectively, which are very similar to that of PFV-HBT. It indicates that the substitution of D* with varied electron-donating ability moiety has almost no effect on the reduction potential of the copolymers and the LUMO energy level is mainly determined by the HBT-based acceptor unit. And the relatively low LUMO energy levels of the copolymers result from the stronger reduction of HBT acceptor unit. On the other hand, the HOMO energy levels of copolymers behave quite differently. The HOMO energy levels of the copolymers PFV-HBT, PPV-HBT, and PTV-HBT are in the range of −5.27 to −4.96 eV, which is clearly affected by the varied electron-donating ability of the three D* due to the modulation of ICT inside the copolymers. Generally, the stronger electron-donating ability donor resulted in a higher HOMO energy level. The electrochemical band gap (E_g^{ec}) was determined to be 1.64 eV for PTV-HBT, 1.75 eV for PPV-HBT, and 1.96 eV for PFV-HBT, which is 0.1–0.2 eV larger than the optically determined ones (E_g^{opt} =1.48–1.83 eV). This difference can be explained by the exciton binding energy of conjugated polymers which is thought to be in the range of 0.1–0.5 eV.[35]

Figure 5 depicts the electron-state-density distribution of the HOMO and LUMO of geometry optimized structures (DFT B3LYP/6-31G*) of analogous monomers PFV-HBT, PPV-HBT, and PTV-HBT using the Gaussium 03 program. To simplify the calculation, only one repeating unit of each polymer was subject to the calculation, with alkyl chains replaced by C_2H_5 groups. The electron density distributions of LUMO levels for

TABLE 2 Optical and Electrochemical Properties of Copolymers

Polymers	$\lambda_{max}^{abs,sol}$ (nm)	$\lambda_{max}^{abs,film}$ (nm)	a (10^4 cm^{-1})	E_g^{opt} (eV)	E_{ox}^{onset} (V)	HOMO (eV)	E_{red}^{onset} (V)	LUMO (eV)	E_g^{ec} (eV)
PFV-HBT	424/553	431/569	7.2	1.83	0.54	−5.27	−1.42	−3.31	1.96
PPV-HBT	451/566	459/578	6.8	1.63	0.34	−5.07	−1.42	−3.31	1.75
PTV-HBT	463/653	475/676	8.7	1.48	0.23	−4.96	−1.41	−3.32	1.64

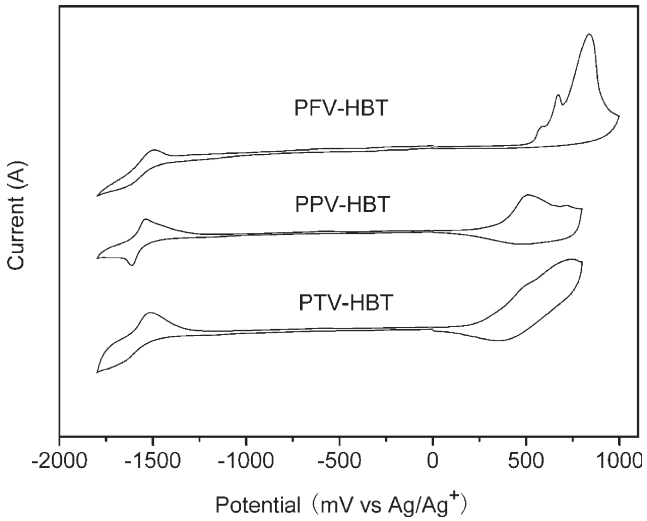

FIGURE 4 Cyclic voltammograms of copolymer thin films on Pt wires in 0.1 M $TBAPF_6$ in acetonitrile. The scan rates used were 50 mV/s.

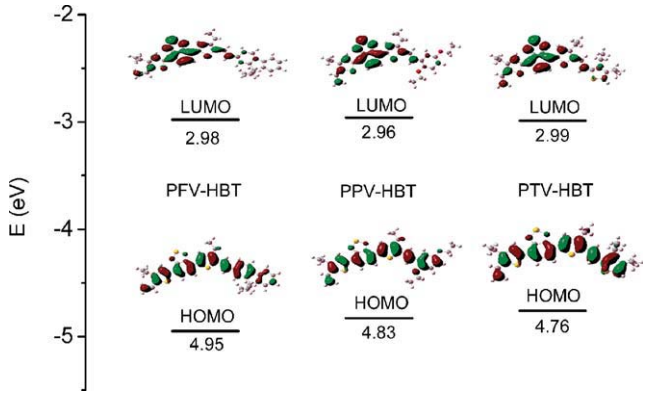

FIGURE 5 DFT-calculated LUMO and HOMO of the geometry optimized structures of analogous monomers of PFV-HBT, PPV-HBT, and PTV-HBT.

these three polymers are nearly identical and primarily localized on the HBT-based acceptor unit. Thus, the change of donor units has almost no effect on the LUMO levels. However, the electron density of HOMO is distributed over the entire conjugated molecule (both the acceptor and donor unit), which indicates the donor unit significantly affects the HOMO level of the resulting polymer. The results from the calculation follow the same trend as we observed from the experimental values.

Photovoltaic Properties

To investigate the photovoltaic properties of the copolymers, the bulk-heterojunction photovoltaic cells with a structure of ITO/PEDOT-PSS/copolymers: PCBM/LiF/Al were fabricated, where the copolymers were used as donors and PCBM as acceptor. The weight ratios between copolymers and PCBM in the active layer have obviously effect on the photovoltaic performance, so BHJ PSCs with varied weight ratios (copolymer:PCBM from 1:1 to 1:4) in the active layers were investigated (the results are list in Table 3). The optimized performances were achieved with weight ratio of copolymers: PCBM at 1:4 (w/w). It is known that solvents used for the preparation of the active layer have a strong impact on the performance of the cell. Here, we chose chlorobenzene as solvent to obtain the copolymer films with good quality.[36] The current-voltage characteristics of the photovoltaic cell based on PFV-HBT:PCBM, PPV-HBT:PCBM, and PTV-HBT:PCBM with weight ratio (1:4 w/w) are shown in Figure 6, and the photovoltac parameters of the photovoltaic cells are summarized in Table 3.

The cell based on PFV-HBT:PCBM (1:4 w/w) showed an open-circuit voltage (V_{oc}) of 0.88 V, a short-circuit current (J_{sc}) 0.95 mA/cm^2, and a fill factor (FF) of 0.39, giving a PCE of 0.33%. The corresponding device parameters of the PSC based on PPV-HBT:PCBM (1:4 w/w) are 0.62 V, 2.12 mA/cm^2, 0.36, and 0.47%, respectively. In comparison with the

TABLE 3 Photovoltaic Properties of the Copolymer Photovoltaic Cells

Donor (Polymer)	Blend Ratio (D:A)	V_{oc} (V)	J_{sc} (mA/cm^2)	FF	PCE (%)	Hole Mobility (cm^2 V^{-1} S^{-1})[a]	Hole Mobility (cm^2 V^{-1} S^{-1})[b]
PFV-HBT	1:1	0.86	0.67	0.30	0.17		
	1:2	0.88	0.71	0.37	0.23		
	1:3	0.88	0.80	0.39	0.27	3.2×10^{-7}	1.6×10^{-6}
	1:4	0.88	0.95	0.39	0.33		
PPV-HBT	1:1	0.60	0.87	0.28	0.15		
	1:2	0.62	1.27	0.30	0.23		
	1:3	0.64	2.02	0.35	0.45	7.5×10^{-8}	9.1×10^{-7}
	1:4	0.62	2.12	0.36	0.47		
PTV-HBT	1:1	0.48	1.02	0.43	0.21		
	1:2	0.50	1.71	0.48	0.41		
	1:3	0.52	2.96	0.49	0.76	8.1×10^{-7}	7.4×10^{-6}
	1:4	0.52	3.98	0.51	1.05		

[a] Measured with polymer-only devices.

[b] Measured with polymer:PCBM (1:4) devices.

device based on PPV-HBT:PCBM, the V_{oc} of the device based on the PFV-HBT:PCBM increases by ca. 0.29 V because the V_{oc} is mainly determined by the energy difference between the HOMO of the donor and the LUMO of the acceptor, and the relatively low-lying HOMO (−5.27 eV) of the PFV-HBT enhances the open circuit voltage.[37,38] The PCE of the device based on PFV-HBT is slightly lower in comparison with that based on PPV-HBT, which is primarily due to a decrease in current density. The higher J_{sc} of the device based on PPV-HBT:PCBM comparing with the device based on PFV-HBT:PCBM could be explained by the broader absorption and lower bandgap of PPV-HBT. Although The V_{oc} (0.52 V) of the PTV-HBT:PCBM (1:4) is smaller than the other two copolymer devices, presumably as a result of the relatively high HOMO level of PTV-HBT, a PCE of 1.05% was still achieved because the increased J_{sc} value of 3.98 mA/cm^2 and FF of 0.51. The device based on PTV-HBT exhibits the highest J_{sc} among the three devices due to the absorbance of PTV-HBT matches the solar radiation better than that of PPV-HBT and PFV-HBT. Furthermore, the amount of the absorbed light depends not only on the edge of absorption wavelength but also on the intensity of the absorption. Comparing the absorption of PFV-HBT, PPV-HBT, and PTV-HBT in Figure 3(b), PTV-HBT have higher absorption coefficient than PFV-HBT and PTV-HBT. That's one of the reasons why the device based on PTV-HBT has the higher J_{sc} than the devices based on PFV-HBT and PPV-HBT. Although PTV-HBT gave the relatively low device performance, the PCE value of 1.05% is still much higher than that (0.13%) of the similar polymer previously reported by Cao and coworkers.[39]

In BHJ solar cells, the hole mobility in the polymer is very important to their photovoltaic performance. We used space charge limited current (SCLC) model to determine the hole mobility in pure copolymers or in blends with PCBM. The devices with a structure of ITO/PEDOT:PSS/ copolymer or copolymer:PCBM (1:4)/Au were fabricated. Figure 7 shows the *J-V* characteristics of the hole-only devices based on PFV-HBT:PCBM, PPV-HBT:PCBM, and PTV-HBT:PCBM. The hole mobility values of copolymers PFV-HBT, PPV-HBT, and PTV-HBT were (see Table 3) estimated according to the equation:

$$J = \frac{9}{8}\varepsilon_r\varepsilon_0\mu_h\frac{(V - V_{bi})^2}{L^3}$$

where V is the applied voltage, J is the current density, ε_r and ε_0 are the relative dielectric constant and the permittivity of the free space (8.85 × 10^{-12} F/m), respectively, μ_h is hole mobility and L is the thickness of the organic layer. The hole mobilities of pure copolymers PFV-HBT, PPV-HBT, and PTV-HBT were estimated to be about 3.2 × 10^{-7} cm^2 V^{-1} s^{-1}, 7.5 × 10^{-8} cm^2 V^{-1} s^{-1}, and 8.1 × 10^{-7} cm^2 V^{-1} s^{-1}, respectively, while that of the blend have increased relative to pure copolymers by ~1 order of magnitude. Obviously, The electron mobility (2 × 10^{-3} cm^2 V^{-1} s^{-1})[40] of PCBM was much higher than the hole mobility of polymer, resulting in an imbalance in the hole and electron transport in the blended film. Because of the poor hole mobility and the imbalance of the hole and electron transport in the blend films of PFV-HBT:PCBM and PPV-HBT:PCBM, the devices were limited to have a low FF values 0.39 and 0.36, respectively, which could be another reason for the lower PCE values of the PFV-HBT:PCBM and PPV-HBT:PCBM.[41]

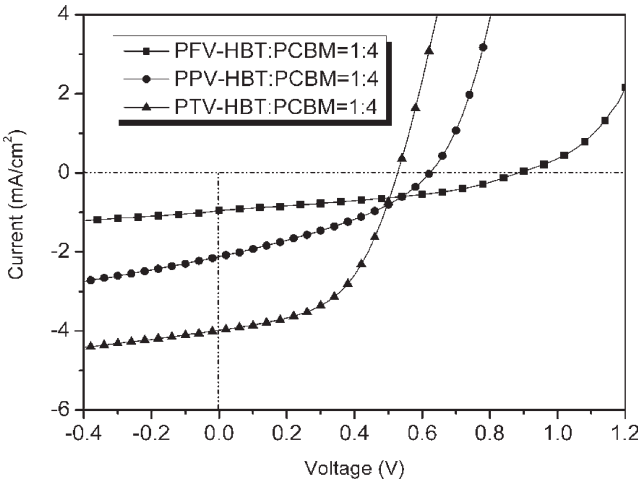

FIGURE 6 *J-V* curves of the copolymer photovoltaic cells based on PFV-HBT, PPV-HBT, and PTV-HBT under the illumination of AM 1.5, 100 mW/cm^2.

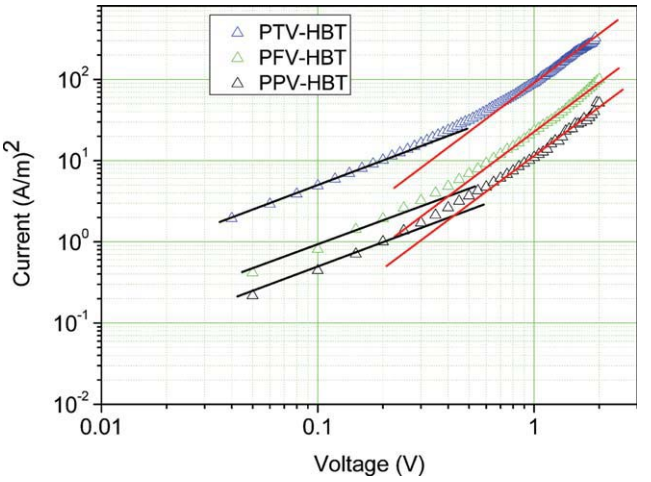

FIGURE 7 *J-V* curve in the dark of an ITO/PEDOT/Copolymers:PCBM/Au device in log axis for log axis for estimating the hole mobility of copolymers. The open triangle symbols are the experimental data. The solid line from 0.05 to 0.60 V means *log J* is fitted linearly dependent on *log V* with a slope of 1. For the solid line from 0.60 to 1 V means *log J* is fitted linearly dependent on *log V* with a slope of 2 (SCLC area). [Color figure can be viewed in the online issue, which is available at wileyonlinelibrary.com.]

CONCLUSIONS

We have synthesized three new low band gap alkylated 4,7-dithien-2-yl-2,1,3-benzothiadiazole (HBT)-based copolymers with vinyl linkages by a Horner cross coupling polymerization. These polymers show strong absorptions in the range of 300–900 nm and have ideal optical bandgaps (1.48–1.83

eV). The HOMO levels of PFV-HBT, PPV-HBT, and PTV-HBT are −5.27, −5.07, and −4.96 eV, respectively, which means that the order of the donor strength is dialkylthiophene > dialkyloxyphenylene > dialkylfluorene. The photovoltaic devices based on the polymers show the PCE in the range of 0.33–1.05%, which indicate that it is an effective way to improve the PCE of photovoltaic devices by adjusting the electron-donating abilities for the type of D-A copolymers.

This work was supported by the State Key Development Program for Basic Research of China (Grant No. 2009CB623605), the National Natural Science Foundation of China (Grant No. 20874035), the 111 Project (Grant No. B06009), and the Project of Jilin Province (20080305).

REFERENCES AND NOTES

1 Yu, G.; Gao, J.; Hummelen, J.; Wudl, F.; Heeger, A. J. Science 1995, 270, 1789–1791.

2 Dennler, G.; Scharber, M. C.; Brabec, C. J. Adv Mater 2009, 21, 1323–1338.

3 Helgesen, M.; Sondergaard, R.; Krebs, F. C. J Mater Chem 2010, 20, 36–60.

4 Krebs, F. C.; Tromholt, T.; Jorgensen, M. Nanoscale 2010, 2, 873–886.

5 Thompson, B. C.; Frechet, J. M. J. Angew Chem Int Ed Engl 2008, 47, 58–77.

6 Gunes, S.; Neugebauer, H.; Sariciftci, N. S. Chem Rev 2007, 107, 1324–1338.

7 Blom, P. W. M.; Mihailetchi, V. D.; Koster, L. J. A.; Markov, D. E. Adv Mater 2007, 19, 1551–1566.

8 Zhang, F. L.; Mammo, W.; Andersson, L. M.; Admassie, S.; Andersson, M. R.; Inganäs, O. Adv Mater 2006, 18, 2169–2173.

9 Zhu, Z. G.; Waller, D.; Gaudiana, R.; Morana, M.; Mulhlbacher, D.; Scharber, M.; Brabec, C. Macromolecules 2007, 40, 1981–1986.

10 (a) Yip, H.-L.; Hau, S. K.; Baek, N. S.; Ma, H.; Gen, A. K.-Y. Adv Mater 2008, 20, 2376–2382; (b) Lee, J. Y.; Choi, M. H.; Song, H. J.; Moon, D. K. J Polym Sci Part A: Polym Chem 2010, 48, 4875–4883; (c) Chen, G. Y.; Lan, S. C.; Lin, P. Y.; Chu, C. W.; Wei, K. H. J Polym Sci Part A: Polym Chem 2010, 48, 4456–4464; (d) Song, S.; Park, S. H.; Jin, Y.; Park, J.; Shim, J. Y.; Kim, I.; Lee, H.; Lee, K.; Suh, H. J Polym Sci Part A: Polym Chem 2010, 48, 4567–4573.

11 Ma, W.; Yang, C.; Gong, X.; Lee, K.; Heeger, A. J. Adv Funct Mater 2005, 15, 1617–1622.

12 Li, G.; Shrotriya, V.; Huang, J.; Yao, Y.; Moriarty, T.; Emery, K.; Yang, Y. Nat Mater 2005, 4, 864–868.

13 (a) Liang, Y. Y.; Wu, Y.; Feng, D. Q.; Tsai, S.-T.; Son, H.-J.; Li, G.; Yu, L. P. J Am Chem Soc 2009, 131, 56–57; (b) Liang, Y. Y.; Feng, D. Q.; Wu, Y.; Tsai, S.-T.; Li, G.; Ray, C.; Yu, L. P. J Am Chem Soc 2009, 131, 7792–7799.

14 (a) Hou, J. H.; Chen, H.-Y.; Zhang, S. Q.; Li, G.; Yang, Y. J Am Chem Soc 2008, 130, 16144–16145; (b) Zou, Y. P.; Najari, A.; Berrouard, P.; Beaupre, S.; Aïch, B. R.; Tao, Y.; Leclerc, M. J Am Chem Soc 2010, 132, 5330–5331; (c) Piliego, C.; Holcombe, T. W.; Douglas, J. D.; Woo, C. H.; Beaujuge, P. M.; Fréchet. J. M. J. J Am Chem Soc 2010, 132, 7595–7597; (d) Padhy, H.; Huang, J. H.; Sahu, D.; Patra, D.; Kekuda, D.; Chu, C. W.; Lin, H. C. J Polym Sci Part A: Polym Chem 2010, 48, 4823–4834; (e) Jung, I. H.; Kim, H.; Park, M. J.; Kim, B.; Park, J. H.; Jeong, E.; Woo, H. Y.; Yoo, S.; Shim, H. K. J Polym Sci Part A: Polym Chem 2010, 48, 1423–1432; (f) Chen, G. Y.; Chiang, C. M.; Kekuda, D.; Lan, S. C.; Chu, C. W.; Wei, K. H. J Polym Sci Part A: Polym Chem 2010, 48, 1669–1675.

15 Chen, H.-Y.; Hou, J. H.; Zhang, S. Q.; Liang, Y. Y.; Yang, G. W.; Yang, Y.; Yu, L. P.; Wu, Y.; Li, G. Nat Photonics 2009, 3, 649–653.

16 (a) Svensson, M.; Zhang, F. L.; Veenstra, S. C.; Verhees, W. J. H.; Hummelen, J. C.; Kroon, J. M.; Inganäs, O.; Andersson, M. R. Adv Mater 2003, 15, 988–991; (b) Chen, M.-H.; Hou, J. H.; Hong, Z. R.; Yang, G. W.; Sista, S.; Chen, L.-M.; Yang, Y. Adv Mater 2009, 21, 4238–4242.

17 (a) Boudreault, P. T.; Michaud, A.; Leclerc, M. Macromol Rapid Commun 2007, 28, 2176–2179; (b) Wang, E. G.; Wang, L.; Lan, L. F.; Luo, C.; Zhuang, W. L.; Peng, J. B.; Cao, Y. Appl Phys Lett 2008, 92, 033307.

18 Liu, C. L.; Tsai, J. H.; Lee, W. Y.; Chen, W. C.; Jenekhe, S. A. Macromolecules 2008, 41, 6952–6959.

19 (a) Blouin, N.; Michaud, A.; Leclerc, M. Adv Mater 2007, 19, 2295–2300; (b) Blounim, N.; Michaud, A.; Gendron, D.; Wakim, S.; Blair, E.; Neagu-Plesu, R.; Durocher, G.; Tao, Y.; Leclerc, M. J Am Chem Soc 2008, 130, 732–742; (c) Chu, T.-Y; Alem, S.; Verly, P. G.; Wakim, S.; Lu, J. P.; Tao, Y.; Beaupré, S.; Leclerc, M.; Bélanger, F.; Désilets, D.; Rodman, S.; Waller, D.; Gaudiana, R. Appl Phys Lett 2009, 95, 063304.

20 (a) Liao, L.; Dai, L. M.; Smith, A.; Durstock, M.; Lu, J. P.; Ding, J. F.; Tao, Y. Macromolecules 2007, 40, 9406–9412; (b) Huo, L. J.; Chen, H.-Y.; Hou, J. H.; Chen, T. L.; Yang, Y. Chem Commun 2009, 37, 5570–5572.

21 Moulé, A. J.; Tsami, A.; Bünnagel, T. W.; Forster, M.; Kronenberg, N. M.; Scharber, M.; Koppe, M.; Morana, M.; Brabec, C. J.; Meerholz, K.; Scherf, U. Chem Mater 2008, 20, 4045–4050.

22 (a) Huo, L. J.; Hou, J. H.; Zhang, S. Q.; Chen, H.-Y.; Yang, Y. Angew Chem Int Ed Engl 2010, 49, 1500–1503; (b) Price, S. C.; Stuart, A. C.; You, W. Macromolecules 2010, 43, 4609–4612.

23 Sonar, P.; Singh, S. P.; Sudhakar, S.; Dodabalapur, A.; Sellinger, A. Chem Mater 2008, 20, 3184–3190.

24 Park, S. H.; Roy, A.; Beaupré, S.; Cho, S.; Coates, N.; Moon, J. S.; Moses, D.; Leclerc, M.; Lee, K.; Heeger, A. J. Nat Photon 2009, 3, 297–302.

25 Liu, B.; Najari, A.; Pan, C.; Leclerc, M.; Xiao, D.; Zou, Y. P. Macromol Rapid Commun 2010, 31, 391–398.

26 Zhang, S. M.; Fan, H. J.; Liu, Y.; Zhao, G. J.; Li, Q. K.; Li, Y. F.; Zhan, X. W. J Polym Sci Part A: Polym Chem 2009, 47, 2843–2852.

27 Ko, S.; Mondal, R.; Risko, C.; Lee, J. K.; Hong, S.; McGehee, M. D.; Bredas, J.-L.; Bao, Z. N. Macromolecules 2010, 43, 6685–6698.

28 Pilgram, K.; Zupan, M.; Skile, R. J Heterocycl Chem 1970, 7, 629–633.

29 Wen, S. P.; Pei, J. N.; Zhou, Y. H.; Li, P. F.; Xue, L. L.; Li, Y. W.; Xu, B.; Tian, W. J. Macromolecules 2009, 42, 4977–4984.

30 Egbe, D. A. M.; Tillmann, H.; Birckner, E.; Klemm, E. Macromol Chem Phys 2001, 202, 2712–2726.

31 Zhou, E. J.; Cong, J. Z.; Yamakawa, S.; Wei, Q. S.; Nakamura, M.; Tajima, K.; Yang, C. H.; Hashimoto, K. Macromolecules 2010, 43, 2873–2879.

32 (a) Yamamoto, T.; Komarudin, D.; Arai, M.; Lee, B. L.; Suganuma, H.; Asakawa, N.; Inoue, Y.; Kubota, K.; Sasaki, S.; Fukuda, T.; Matsuda, H. J Am Chem Soc 1998, 120, 2047–2058; (b) Yue, W.; Zhao, Y.; Tian, H. K.; Song, D.; Xie, Z. Y.; Yan, D. H.; Geng, Y. H.; Wang, F. S. Macromolecucules 2009, 42, 6510–6518.

33 Peng, Q.; Park, K.; Lin, T.; Durstock, M.; Dai, L. M. J Phys Chem B 2008, 112, 2801–2808.

34 Wen, S. P.; Pei, J. N.; Zhou, Y. H.; Xue, L. L.; Xu, B.; Li, Y. W.; Tian, W. J. J Polym Sci Part A: Polym Chem 2009, 47, 1003–1032.

35 Zhu, Y.; Champion, R. D.; Jenekhe, S. A. Macromolecules 2006, 39, 8712–8719.

36 Shaheen, S. E.; Brabec, C. J.; Sariciftci, N. S. Appl Phys Lett 2001, 78, 841.

37 Scharher, M. C.; Mühlbacher, D.; Koppe, M.; Denk, P.; Waldauf, C.; Heeger, A. J.; Brabec, C. J. Adv Mater 2006, 18, 789–794.

38 Hou, J. H.; Park, M-H.; Zhang, S. Q.; Yao, Y.; Chen, L. M.; Li, J-H.; Yang, Y. Macromolecules 2008, 41, 6012–6018.

39 Xia, Y. J.; Deng, X. Y.; Wang, L.; Li, X. Z.; Zhu, X. H.; Cao, Y. Macromol Rapid Commun 2006, 27, 1260–1264.

40 Mihailetchi, V. D.; van Duren, J. K. J.; Blom, P. W. M.; Hummelen, J. C.; Janssen, R. A. J.; Kroon, J. M.; Rispens, M. T.; Verhees, W. J. H.; Wienk, M. M. Adv Funct Mater 2003, 13, 43–46.

41 Hou, J. H.; Chen, T. L.; Zhang, S.; Chen, H.-Y.; Yang, Y. J Phys Chem C 2009, 113, 1601–1605.